

In Vitro and In Vivo Metabolism of a Novel Antimitochondrial Cancer Metabolism Agent, CPI-613, in Rat and Human

Vijay Bhasker Reddy, Lakmal Boteju, Asela Boteju, Li Shen, Kelem Kassahun, Nageshwar Reddy, Adrian Sheldon, Sanjeev Luther, and Ke Hu

Rafael Pharmaceuticals, Cranbury, New Jersey (V.B.R., L.B., A.B., N.R., S.L., K.H.); Frontage Laboratories, Exton, Pennsylvania (L.S., K.K.); and Charles River Laboratories, Worcester, Massachusetts (A.S.)

Received October 11, 2021; accepted January 20, 2022

ABSTRACT

CPI-613, an inhibitor of pyruvate dehydrogenase (PDH) and α -ketoglutarate dehydrogenase (KGDH) enzymes, is currently in development for the treatment of pancreatic cancer, acute myeloid leukemia, and other cancers. CPI-613 is an analog of lipoic acid, an essential cofactor for both PDH and KGDH. Metabolism and mass balance studies were conducted in rats after intravenous administration of [14 C]-CPI-613. CPI-613 was eliminated via oxidative metabolism followed by excretion of the metabolites in feces (59%) and urine (22%). β -Oxidation was the major pathway of elimination for CPI-613. The most abundant circulating components in rat plasma were those derived from β -oxidation. In human hepatocytes, CPI-613 mainly underwent β -oxidation (M1), sulfur oxidation (M2), and glucuronidation (M3). The Michaelis-Menten kinetics (V_{\max} and K_m) of the metabolism of CPI-613 to these three metabolites predicted the fraction

metabolized leading to the formation of M1, M2, and M3 to be 38%, 6%, and 56%, respectively. In humans, after intravenous administration of CPI-613, major circulating species in plasma were the parent and the β -oxidation derived products. Thus, CPI-613 metabolites profiles in rat and human plasma were qualitatively similar. β -Oxidation characteristics and excretion patterns of CPI-613 are discussed in comparison with those reported for its endogenous counterpart, lipoic acid.

SIGNIFICANCE STATEMENT

This work highlights the clearance mechanism of CPI-613 via β -oxidation, species differences in their ability to carry out β -oxidation, and subsequent elimination routes. Structural limitations for completion of terminal cycle of β -oxidation is discussed against the backdrop of its endogenous counterpart lipoic acid.

Introduction

CPI-613 is a first-in-class antimitochondrial cancer metabolism agent, currently in development for the treatment of pancreatic cancer (PANC), acute myeloid leukemia (AML), and other cancers (Alistar et al., 2017; Pardee et al., 2019; Philip et al., 2019). The profoundly altered metabolism of tumor cells has recently emerged as one of the most promising new domains for therapeutic targeting of cancer (Hammoudi et al., 2011; Vander Heiden, 2011; DeBerardinis and Chandel, 2016; Missirololi et al., 2020). CPI-613 is a stable analog of normally transient, acylated catalytic intermediates of lipoic acid, an essential cofactor for both the pyruvate dehydrogenase (PDH) and α -ketoglutarate dehydrogenase (KGDH) enzyme complexes (Bingham et al., 2014; Stuart et al., 2014; Alistar et al., 2017). CPI-613 inactivates PDH in tumor cells by hyperactivating the corresponding regulatory pyruvate dehydrogenase kinases (PDKs), which phosphorylate and inactivate PDH (Zachar et al., 2011). CPI-613 simultaneously inactivates KGDH by hyperactivating a redox feedback loop normally controlling the

enzyme's activity (Stuart et al., 2014). The simultaneous inhibition of these two tricarboxylic acid (TCA) cycle enzymes dramatically compromises mitochondrial metabolic flows, triggering multiple, redundant cell death pathways (Vander Heiden, 2011; Zachar et al., 2011; Bingham et al., 2014; Stuart et al., 2014; DeBerardinis and Chandel, 2016).

CPI-613 has demonstrated time- and dose-dependent in vitro activity in a broad range of cancer cells, including solid and hematologic malignancy-derived cell lines (Zachar et al., 2011; Pardee et al., 2016). CPI-613 treatment resulted in a dose-dependent increase in phosphorylation of the E1 subunit of PDH, inhibiting PDH in tumor cell lines, including solid tumors and hematologic malignancies (Zachar et al., 2011; Pardee et al., 2019; Stuart et al., 2014). CPI-613 also inhibits basal and maximal mitochondrial respiration in tested pancreatic (PANC-1, AsPC-1), and colorectal (LoVo, SW620) cell lines. In permeabilized PANC-1 cells, CPI-613 blocks only pyruvate and α -ketoglutarate (complex I substrates)-driven mitochondrial respiration, whereas succinate (complex II substrate)-driven respiration remains unaffected (internal data to be published). These results are consistent with the principle of PDH and α -KGDH as the key mitochondrial targets of CPI-613.

The objective of the current study was to evaluate the pharmacokinetics (PK), metabolism, and excretory mass balance of [14 C]-CPI-613 in Sprague Dawley (SD) rats and the metabolism pathways in humans. The ultimate goal was to identify the circulating metabolites in rats and compare with those circulating metabolites in humans to ensure that

This work received no external funding.

V.B.R., L.B., A.B., N.R., J.H., and S.L. are paid employees of Rafael Pharmaceuticals Inc. L.S., K.K., and A.S. are paid employees of contract research organizations Frontage Laboratories or Charles River Laboratories.

dx.doi.org/10.1124/dmd.121.000726.

ABBREVIATIONS: ACN, acetonitrile; AUC, area under the curve; CID, collision-induced dissociation; CL, clearance; CoASH, coenzyme A; C-S, carbon-sulfur; D5W, 5% dextrose in water; FA, formic acid; f_m , fraction metabolized; HPLC, high-performance liquid chromatography; JVC, jugular vein catheter; KGDH, α -ketoglutarate dehydrogenase; LC-MS, liquid chromatography-mass spectrometry; LC-MS/MS, liquid chromatography-tandem mass spectrometry; LSC, liquid scintillation counting; M, metabolite; m/z, mass- to-charge ratio; P450, cytochrome P450; PANC, pancreatic cancer; PDH, pyruvate dehydrogenase; PK, pharmacokinetics; SD, Sprague Dawley; TEA, triethanolamine.

they were adequately tested for safety in preclinical species. The metabolism profiles and excretion patterns of CPI-613 are discussed against the backdrop of its endogenous counterpart lipoic acid.

Materials and Methods

CPI-613 was synthesized at PCI Synthesis (Newburyport, MA). The β -oxidation metabolite M1 was synthesized at Princeton Global Synthesis (Ewing, NJ). Metabolites M2 (sulfoxide) and M3 (glucuronic acid conjugate) were synthesized at Rafael Pharmaceuticals (Cranbury, NJ). [^{14}C]-CPI-613 was synthesized at Pharmaron (Cardiff, UK). The ^{14}C label was located on both benzylic carbons. The specific activity of [^{14}C]-CPI-613 was 56.6 mCi/mmol, the chemical purity was 99.4%, and the radiochemical purity was 98.9%, as determined by high-performance liquid chromatography (HPLC). Triethanolamine was purchased from Spectrum Chemical Manufacturing Corp (New Brunswick, NJ). Hippuric acid, dextrose, triton X-405, and sodium hydroxide were purchased from Sigma or other sources. Carbo-Sorb E, PermaFluor E⁺, Hionic-Fluor, Ultima Gold, and Ultima-Flo M liquid scintillation cocktails were obtained from Perkin Elmer Life Sciences (Waltham, MA). Stopflow AQ liquid scintillation cocktail was obtained from AIM research company (Hockessin, DE). Ethanolamine, 2-methoxyethanol, and solvents used for chromatographic analysis were HPLC or American Chemical Society (ACS) reagent grade and purchased from Fisher (Fair Lawn, NJ) or another commercial supplier. All other reagents were of analytical or ACS reagent grade. Pooled, mixed-gender human cryopreserved hepatocytes ($n = 10$; batch #XZI) were purchased from BioIVT (Baltimore, MD). Valproic acid, coenzyme A (CoASH), ATP, L-carnitine, MgCl_2 , and potassium phosphate buffer were obtained from Sigma-Aldrich (St. Louis, MO) or other commercial suppliers. Human liver mitochondria were purchased from XenoTech LLC (Lenexa, KS).

Mass Balance Studies in SD Rats. Excretion mass balance of [^{14}C]-CPI-613 in male SD rats after a single intravenous dose was conducted at Frontage Laboratories (Exton, PA). The study was conducted in compliance with Frontage Institutional Animal Care and Use Committee protocols.

Experimental Animals and Surgeries. Adult male SD rats (8–12 weeks old) were obtained from Charles River Breeding Laboratories. A total of seven rats were used and divided into two groups (Table 1). Body weights of each rat at the time of dosing were in the range of 277–387 g. The four rats in group 1 were surgically implanted with jugular vein catheter (JVC) for intravenous infusion and with femoral artery catheter for blood collection at least 2 days prior to dosing. The three rats in group 2 were surgically implanted only with jugular vein catheter (JVC) for intravenous infusion. Animals were not fasted prior to intravenous dosing. All animals had at least 3 days of acclimation after receipt at the vivarium prior to dosing. During acclimation, all animals were housed in polycarbonate cages on contact bedding (Alpha Dry, Animal Specialties and Provisions, Quakertown, PA) with no more than three animals per cage. After the radiolabeled dose was administered, the animals were placed into individual plastic metabolism cages with wire flooring or on contact bedding. Certified Purina Powdered Rodent #5002 Diet (Animal Specialties and Provisions) or DietGel76A and HydroGel (ClearH₂O, Portland, ME) were offered ad libitum during the study. Reverse osmosis filtered water was provided in sanitized bottles ad libitum to animals during the acclimation and testing periods.

Dosing Regimen, Sample Collection, and Storage. The stock solution of [^{14}C]-CPI-613 was prepared at 50 mg/ml in 1M triethanolamine (TEA) and diluted to the desired concentration with 5% dextrose in water. [^{14}C]-CPI-613 was intravenously infused for 2 hours at 100 mg/kg (~200 $\mu\text{Ci/kg}$, 5 ml/h per kg) using the dosing regimen as shown in Table 1. Prior to dosing, the body weights of animals were recorded. Syringe weights were recorded before and

after dosing. Four intact rats in group 1 were dosed and feces, urine, cage rinse, and serial blood samples were collected at predetermined time points/intervals up to 168 hours. Blood and plasma were collected at 0.083, 0.5, 1, 2, 2.5, 3, 4, 8, 12, 24, 48, and 168 hours. Urine was collected at predose, 0–6 hours, 6–24 hours, and daily up to 168 hours. Feces were collected at predose and daily up to 168 hours. Cage rinse with 25% ethanol in water was collected at the end of 168 hours. Whole blood samples were collected into K₂EDTA tubes and pooled, and then aliquot (~200 μl) was used to obtain plasma after centrifugation. For the three intact rats in group 2, expired air was collected by using two validated carbon dioxide trapping apparatus, which were equipped with airflow apparatus (Columbus Instruments International Corporation, Columbus, OH). Exhaled [^{14}C] CO₂ was trapped for up to 144 hours postdose by using a mixture of ethanolamine: 2-methoxyethanol (1:3, v/v) in two traps in series (~150 ml for each). The total radioactivity in absorbent of expired CO₂ samples was analyzed by liquid scintillation counting (LSC) after collection. At the end of in-life phase, rats were sacrificed by overdose of CO₂. Each cage was rinsed thoroughly with 25% ethanol in water and collected in a separate container for total radioactivity. All samples, except for blood and plasma, were weighed after collection before storing. Plasma, urine, and feces were stored at -70°C . Residual carcasses were stored at -20°C . Whole blood and cage rinse samples, as well as the absorbent of expired air samples, were stored at 4°C .

Measurement of Total Radioactivity in Samples. Duplicate aliquots of diluted dose solutions (~200 μl), diluted dose wipes (~500 μl), urine (~200 μl), cage rinse (~500 μl), and singlet of plasma (~20 μl at early time points and higher volumes at later time points) were mixed with Ultima Gold (5 ml) as scintillation fluid and analyzed for radioactivity concentrations by LSC. Fecal samples were homogenized in approximately 5-fold volume of purified water. Duplicate aliquots of fecal homogenates (~200 μl) and whole blood samples (~40 μl or higher) were transferred to Combusto Cones and combusted using a Sample Oxidizer (Model A307, Perkin Elmer) equipped with an Oximate 80 Robotic Automatic Sampler. The weights of each aliquot were recorded. The [^{14}C]-CO₂ generated from the combusted samples was trapped in Carbo Sorb E (~7 ml) in 20 ml liquid scintillation vials, and radioactivity was determined with PermaFluor E+ (~8 ml) as the scintillant using a Tri-Carb LSC. The radioactivity in each sample was used to calculate total radioactivity concentrations and percentage of the dose.

All four rats received [^{14}C]-CPI-613 intravenous dose in group 1 and were analyzed for total radioactivity remaining in carcasses. Rat carcasses were weighed and solubilized at 40°C for about 96 hours in a solution containing sodium hydroxide (~80 g), triton X-405 (100 ml), distilled water (600 ml), and 300 ml of methanol. Aliquots of the digests (~0.3 ml) in triplicates were weighed and then burned with oxidizer followed by determination of radioactive content by LSC. Carcass digests were retained at room temperature. Total radioactivity in carcasses was calculated for mass balance of dosed radioactivity. For radioactivity in expired air, duplicate aliquots (~1 ml) of the mixture of expired carbon dioxide absorbents were mixed with 5 ml of Hionic-Fluor for radioactivity measurement by LSC.

Sample Preparation for Metabolite Analysis in Rat Plasma, Urine, and Fecal Homogenate. Plasma samples were pooled by equal volume at each time point across each animal, and then one pooled plasma sample was prepared by Hamilton method across time points up to 48 hours. One aliquot of the pooled plasma sample (225 μl) was extracted with acetonitrile (ACN) (600 $\mu\text{l} \times 2$) by vortex mixing. The supernatant obtained after centrifugation was dried under a stream of nitrogen. The dried residue was reconstituted in 200 μl of 30% ACN in water and centrifuged at 14,000 rpm for 10 minutes at 4°C . The clear supernatant was analyzed by liquid chromatography-mass spectrometry (LC-MS).

TABLE 1
Study design of [^{14}C] CPI-613 mass balance in male Sprague Dawley Rats

GroupNumber	Number of Rats	Dose Route	DoseRegimen	Target Dose Concentration and Volume				
				$\mu\text{Ci/kg}$	mg/kg	$\mu\text{Ci/ml}$	mg/ml	ml/kg
Group 1	4 (JVC/FAC)	2-hr i.v.infusion	Day 1	~200	100	20	10	10
Group 2	3 (JVC)	2-hr i.v.infusion	Day 1	~200	100	20	10	10

FAC, femoral artery catheter.

Urine sample was pooled across animals (2 ml per animal) to generate one pooled sample representing >90% of excreted urine radioactivity. The pooled urine sample was extracted with acetonitrile, concentrated, and analyzed by LC-MS as described above.

Fecal samples were pooled across animals in similar ways to the urine sample to generate one pooled sample representing >90% of excreted fecal radioactivity. Aliquot (~0.3 g) was extracted with 3-fold volumes of acetonitrile twice by vortex mixing, sonication, and centrifugation. The supernatants were combined and dried down under a stream of nitrogen. Residue was reconstituted in 100 μ l of DMSO and was injected into HPLC with ultraviolet spectroscopy and radioactivity detection for metabolite profiles, and radioactive metabolites were identified by liquid chromatography-tandem mass spectrometry (LC-MS/MS).

CPI-613 Metabolism in Human Plasma. The human plasma samples used in the present study were obtained from an investigator sponsored phase I trial conducted at Atlantic Health Systems (Morristown, NJ) by Dr. Angela Alistar (study details and results to be published separately). Briefly, it was a single-center, single-arm, open-label study in locally advanced or metastatic pancreatic cancer patients (total 21 subjects: eight males, 13 females; aged 56–80 years). CPI-613 dosing solution was prepared from 50 mg/ml in triethanolamine stock solution and diluted to a desired concentration with 5% dextrose in water. CPI-613 was administered at 500, 1000, and 1500 mg/m² by i.v. infusion at ~2–4 ml/min for 0.5–2 hours on days 1, 8, and 15, respectively. The plasma samples collected at 0, 0.25, 0.5, 1, 1.5, 2, 2.5, 3, and 4 hours after the start of 1500 mg/m² infusion in nine subjects (seven males, two females) were used in the present study. The pooled plasma samples (1–4 hours, pooled by volume) were individually extracted with four volumes of ACN and centrifuged to precipitate proteins. Equal volumes of the supernatants from nine subjects were pooled for LC-MS analysis. Predose samples from the same study subjects were used as a control.

Kinetics of CPI-613 Metabolism in Human Hepatocytes and Fraction Metabolized. Kinetics of CPI-613 metabolism in human hepatocytes by following the metabolites M1 (β -oxidation), M2 (sulfoxide), and M3 (glucuronidation) were conducted at Frontage Laboratories (Exton, PA). Prior to the main experiment, linear conditions for the metabolite formation were determined. Human cryopreserved hepatocytes were thawed in a 37°C water bath with gentle shaking until the ice almost melted. The suspension was immediately transferred to a centrifuge tube (50 ml) containing prewarmed thawing media at 37°C with gentle handshaking to prevent the cells from settling. The cell suspension was centrifuged at 50 \times g for 5 minutes at 4°C. The supernatant was discarded, and the pellets were resuspended in prewarmed incubation media (5 ml) at 37°C. The percentage of viable cells in the suspension were determined by using the Trypan Blue stain method to ensure a viability of >70%. CPI-613 (10 μ M) was incubated using various incubation times (10, 20, 30, 60, 120, 180, and 240 minutes) and human hepatocyte densities (0.2, 0.4, 0.8, and 1 million cells/ml). Incubations were conducted in a 24-well plate containing human hepatocyte suspensions at 37°C under 5% CO₂ and 95% air. Aliquots were removed in duplicate at the designated times, and the reactions were stopped by addition of ACN (three volumes containing 200 ng/ml warfarin as the internal standard). The samples were centrifuged at 16,000 \times g for 10 minutes at 4°C, and 100 μ l of the supernatant was transferred to a 96-well plate containing 100 μ l of water. Samples were vortex-mixed for 5 minutes and aliquots of the supernatant were analyzed for M1, M2, and M3 by LC-MS/MS using the peak area approach.

For Michaelis-Menten kinetic determination, CPI-613 was incubated at various concentrations (1, 2.5, 5, 10, 25, 50, 100, 200, 500, and 1000 μ M) using the optimized incubation time (135 minutes) and hepatocyte density (0.4 million cells/ml). Incubations were carried out in triplicate using incubation conditions as described above. 7-Hydroxycoumarin and midazolam were included as positive control to confirm the viability of the hepatocytes. Samples were then processed in the same manner as described above for standards and quality control samples, and the formation of M1, M2, and M3 was monitored.

CPI-613 Incubations with Liver Microsomes. CPI-613 (1 and 10 μ M) was incubated with rat and human liver microsomes (0.5 mg/ml in 0.1 M potassium phosphate buffer containing 1 mM EDTA, pH 7.2) at 37°C for 0, 15, 30, 60, and 120 minutes. Incubations were initiated by the addition of NADPH (1 mM) and terminated by the addition of acetonitrile containing deuterated CPI-613 internal standard. Samples were vortex mixed and centrifuged at 1400 \times g for 5 minutes at ambient temperature. Supernatants were removed from the microsome pellets and stored at –20°C until analysis by LC-MS. Control

incubations were conducted by incubating CPI-613 (1 and 10 μ M) in microsomes in the absence of NADPH at all time points to determine the stability of the test article under the incubation conditions.

CPI-613 Incubations with Human Liver Mitochondria. Experimental conditions for mitochondrial incubations were as described before (Kassahun et al., 1994). The reaction mixture contained CPI-613 (10, 50, or 100 μ M) pooled human liver mitochondria (5 mg/ml), phosphate buffer (0.1 M, pH 7.4), ATP (5 mM), CoASH (0.1 mM), L-carnitine (2 mM), and MgCl₂ (3 mM). The incubations were carried out for 2 hours, and aliquots (300 μ l) were taken at 0.5, 1, and 2 hours. The reactions were terminated with ACN (900 μ l), the samples were centrifuged for 10 minutes (4000 \times g, 4°C), and the supernatants were transferred to glass tubes, dried under stream of nitrogen at room temperature. The dried residue was reconstituted with 200 μ l of 25% aqueous ACN and stored at –80°C until analysis by LC-MS/MS. Valproic acid (1000 μ M) was used as the positive control (Silva et al., 2008). The incubation conditions were modified to ensure optimal β -oxidation as confirmed with the metabolism of valproic acid. Incubations that lacked ATP, CoASH, and L-carnitine served as negative control.

Instrumentation

Analyses in Rat Mass Balance Studies. The analyses of radiochemical purity of [¹⁴C] CPI-613 stock solution, dose formulation, and extracts for metabolite profiles of [¹⁴C] CPI-613 in pooled plasma, urine, and feces were performed using HPLC coupled to radioactive detector. The integrated system consisted of Dionex Ultimate UHPLC 3000 or Shimadzu UHPLC with binary pumps, autosampler, and radioactivity detectors. The radioactive detector ARC3 (AIM Research Company) equipped with a 250- μ l flow cell was used for stock and dose purity check. The radioactive detector β -RAM4 equipped with a 100- μ l flow cell was used for metabolite profiling. StopFlow AQ (ARC3) and Ultima Flo (β -RAM4) were used as scintillation cocktail for liquid chromatography/radioactivity detection. Separation of metabolites was achieved on a 5- μ m Phenomenex Luna C18 column (2 \times 250 mm). Mobile phase A consisted of water and B of acetonitrile, and both contained 0.1% formic acid (FA). The column was eluted at a flow rate of 0.3 ml/min using a stepwise gradient from 5% to 27% B at 28 minutes, 50% B at 75 minutes, and 95% B at 100 minutes. One-fourth of the column eluate was directed into the mass spectrometer and the remainder into a β -Ram radiometric detector. The Orbitrap-Elite mass spectrometer was equipped with an electrospray ionization source and operated in positive ionization mode. The spray voltage was maintained at 3 kilovolts, and the capillary temperature was set at 300°C. Full scan spectra, mass-to-charge ratio (*m/z*) 100 to 1500, were obtained in the positive ion electrospray mode, and product ion spectra were generated by collision-induced dissociation (CID) of MH⁺ ions of interest. The CID of MH⁺ was achieved with nitrogen as the collision gas at the collision energy of 35 electron volts.

Metabolite Analysis in Human Plasma. CPI-613 and its metabolites in human plasma were identified using Waters Acquity UPLC system coupled to a Waters XevoTQ LC-MS instrument equipped with electrospray ionization and operated in positive ion mode. Metabolites were separated on UPLC column (BEH C18, 2.1 \times 50 mm, 1.7 μ m) at 40°C oven temperature. The mobile phase consisted of ACN:Water, 95:5, 0.1% FA (A) and ACN:Methanol, 75:25, 0.1% FA (B). The column was eluted using a linear gradient from 5% to 95% B in 20 minutes at a flow rate of 0.25 ml/min. Data were captured and processed using MassLynx v.4.1 (LC-MS/MS) software.

Metabolite Analysis and Quantitation in Human Hepatocytes. Aliquots of the hepatocyte extracts were analyzed for CPI-613, M1, M2, and M3 by an LC-MS/MS method. A rapid LC-MS/MS method using a method that was developed in accordance with FRONTAGE Tier 2 non-GLP bioanalytical assay standard operating procedure. Tier 2 assay consists of two separate standard curves, one placed at the

beginning of the analytical run and the other arranged toward the end of the sample analysis. Three levels of quality control (low, medium, and high) were used to ensure reliability of the assay. Analysis was carried out on a Sciex API 4000 mass spectrometer interfaced with a Shimadzu HPLC system. Separation was achieved using an ACE Excel5 C18 (50 × 2.1 mm) column with a mobile phase A consisting of water and B of acetonitrile, and both contained 0.1% formic acid. The column was eluted using a linear gradient from 0% to 95% B in 4.5 minutes at a flow rate 0.5 ml/min. The mass spectrometer was operated in the positive ion mode using multiple reaction monitoring (MRM) with the following precursor/product ion pairs: m/z 389 → 265.1, 361 → 237.2, 405 → 265.1, 565 → 265.1 (for CPI-613, M1, M2, and M3, respectively) and m/z 309 → 163 (warfarin, internal standard).

Metabolite Analysis in Liver Microsomes. Metabolite analysis in incubations with liver microsomes was carried out on a Sciex API 5000 mass spectrometer interfaced with a Shimadzu HPLC system. Separation was achieved using a Waters Xbridge C18 5 μ m (30 × 2.1 mm) column with a mobile phase A consisting of water and B of acetonitrile, and both contained 0.1% formic acid. The column was eluted using a linear gradient from 40% to 95% B in 1.1 minutes at a flow rate 1 ml/min. The mass spectrometer was operated in the negative ion mode using multiple reaction monitoring (MRM) with the following precursor/product ion pairs: m/z 387.1 → 123 for CPI-613, m/z 402.8 → 312.2 for M2, and m/z 359.2 → 123 for M1.

Metabolite Analysis in Liver Mitochondria. Metabolite profiling and identification were performed using an Agilent HPLC 1200 system (pumps, autosampler, and photodiode array) coupled to an LTQ-Orbitrap mass spectrometer. Separation was achieved on a Phenomenex Luna C18 (2) column (2.0 × 250 mm, 5 μ m) using a mobile phase consisting of 0.05% trifluoroacetic acid in water and 0.05% trifluoroacetic acid in ACN with a step gradient from 5% to 30% B in 3 minutes and then to 95% B in 25 minutes. The LTQ-Orbitrap mass spectrometer was equipped with an electrospray ionization interface and was operated in the positive ionization mode. Mass spectra were acquired in full scan (mass-to-charge ratio m/z 100 to 730) and data-dependent scan sequential mass spectrometry ($n = 4$) modes. The spray voltage was maintained at +5.0 kilovolts, and the capillary temperature was set at 350°C. Product ion spectra were generated by collision-induced dissociation (CID) of MH^+ ions of interest. The CID of MH^+ was achieved with nitrogen as the collision gas at the collision energy of 35 electron volts. Xcalibur (version 2.1.0) was used to acquire mass spectral data. It was also used to control the various components of Agilent-LTQ-Orbitrap system.

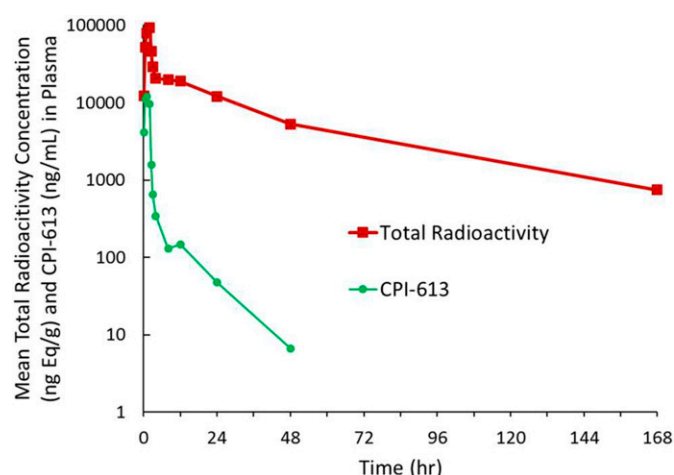


Fig. 2. Mean concentration-time profiles of CPI-613 and total radioactivity in plasma after infusion of a single i.v. dose of 100 mg/kg (200 μ Ci/kg) [14 C] CPI-613 to SD rats ($n = 4$). Radioactivity in plasma was determined by liquid scintillation counting; plasma concentrations of CPI-613 were determined by LC-MS.

Results

[14 C] CPI-613 Excretion Mass Balance in Rats. After a single i.v. infusion at 100 mg/kg (200 μ Ci/kg) of [14 C] CPI-613 in rats, the mean cumulative percent of dose recovered in excreta is shown in Fig. 1. Radioactivity was excreted gradually, and the majority (81%) of it was recovered within the 168-hour collection period. The radioactivity recovered in feces and urine was 59% and 22%, respectively. Only a small percentage (<0.01%) of the dose was recovered in cage rinse. It appeared that the total dosed radioactivity was not completely excreted even 168 hours postdose. On day 7 alone, about 3% of the dose was found in excreta (urine and feces). Therefore, all four carcasses at 168 hours were analyzed for any remaining radioactivity. The recovery of radioactivity in carcasses was 5% of the dose. Adding all radioactivity found in excreta and carcasses, the total recovery of [14 C]-CPI-613-related radioactivity was $86\% \pm 3.6\%$ of the dose.

Expired air was collected from three separate rats (group 2) after the same 2-hour i.v. infusion of [14 C]-CPI-613 at 100 mg/kg. Expired [14 C]-CO₂ was trapped for up to 144 hours postdose. Approximately 1% of the administered total radioactivity was recovered in expired air within 48 hours postdose. With increased CO₂ collection time up to 144 hours, the total recovery in expired air was still 2.3% of the dose. Based on these data, although [14 C]-CPI-613 was excreted through expired air, it was not a major excretion pathway for [14 C]-CPI-613 in rats.

Pharmacokinetics of CPI-613 and Total Radioactivity in Rat Plasma. After a single i.v. infusion of [14 C]-CPI-613 at 100 mg/kg, the time courses of CPI-613 and total radioactivity in pooled plasma of rats are shown in Fig. 2. Pharmacokinetic parameters of total radioactivity and CPI-613 are shown in Table 2. CPI-613 showed high clearance (CL) of 61 ml/min per kg and moderate to high volume of distribution

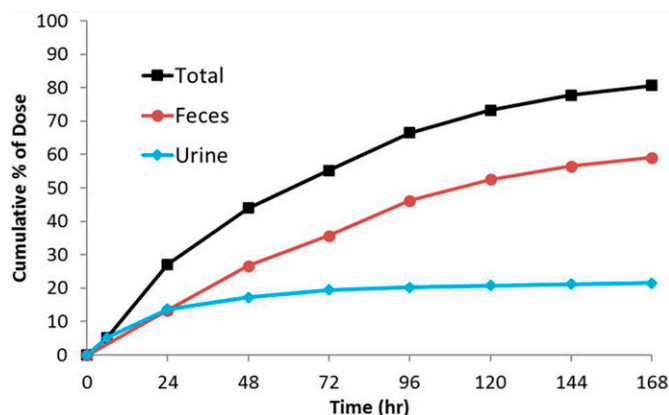


Fig. 1. Mean percent of the radioactive dose recovered in urine and feces with time after infusion of a single i.v. dose of 100 mg/kg (200 μ Ci/kg) [14 C] CPI-613 to SD rats ($n = 4$). Radioactivity in fecal homogenates and urine was determined at Frontage Laboratories and expressed as percentage of administered dose.

TABLE 2

Mean plasma PK of total radioactivity or CPI-613 after a 2-hour i.v. infusion of 100 mg/kg [14 C] CPI-613 (~200 μ Ci/kg) to Sprague Dawley rats

Compound	$t_{1/2}$ (h)	T_{max} (h)	C_{max} (ng/ml) ^a	AUC_{Inf} (h*ng/ml) ^a	V_{ss} (l/kg)	CL (ml/min per kg)
TRA ^b	34.0	2.00	93,300	1,160,000	3.0	1.4
CPI-613	8.1	1	12,000	27,200	7.2	61

^a $t_{1/2}$, half-life; T_{max} , time at which maximal concentration was observed.

^afor radioactivity ng-Eq/ml and h*ng-Eq/ml; mean values ($n = 4$)

^btotal radioactivity

(V_d) of 7.2 l/kg. The elimination half-life of CPI-613 was ~8 hours. The mean C_{max} and area under the curve (AUC)_{0–inf} values in plasma were 12,000 ng/ml and 27,200 hours*ng/ml, respectively. In contrast, clearance of total radioactivity was low (1.4 ml/min per kg) with moderate volume of distribution (3 l/kg). The elimination half-life of total radioactivity was long at 34 hours. The mean C_{max} and AUC_{inf} values for plasma total radioactivity were 93,300 ng Eq/ml and 1,160,000 hours*ng Eq/ml, respectively. The ratio of AUC_{0–inf} value of the unchanged CPI-613 to that of the total radioactivity in plasma was about 0.023 in rats, suggesting that CPI-613 is highly metabolized in rat plasma. The ratio of AUC_{0–inf} value of the total radioactivity in blood to plasma was 0.69, which suggests the limited partition of the radioactivity to red blood cells in rat plasma.

Identification of Metabolites by LC-MS/MS. The structures of CPI-613 metabolites were established by LC-MS/MS analysis. The fragmentation spectra of CPI-613 and the metabolites are presented in Table 3.

Mass Spectra of CPI-613. The protonated molecular ion of CPI-613 was observed at m/z 389.1603. Loss of H_2O from the m/z 389 gave the fragment ion at m/z 371. Cleavage at C-S bonds at various positions gave fragment ions at m/z 265, 181, 173, and 91. Loss of H_2O from m/z 173 gave a fragment ion at m/z 155. The benzyl(methyl)sulfane moiety of the compound corresponded to the fragment ion at m/z 137. The mass spectra and fragmentation ions of CPI-613 observed in plasma were the same as the mass spectra of reference standard CPI-613.

Mass Spectra of M1. The protonated molecular ion of M1 was observed at m/z 361.1285. Loss of H_2O from the m/z 361 gave the fragment ion at m/z 343. Cleavage at carbon-sulfur (C-S) bonds at various positions gave fragment ions at m/z 237 and 181. The mass spectra and fragmentation ions of M1 observed in plasma were the same as the mass spectra of reference standard.

Mass Spectra of M2. The protonated molecular ion of M2 was observed at m/z 405.1544. Loss of H_2O from the m/z 405 gave the fragment ion at m/z 387. Cleavage at C-S bonds at various positions gave fragment ions at m/z 265, 173, and 91. Loss of H_2O from the m/z 173 gave a fragment ion at m/z 155. The mass spectra and fragmentation ions of M2 observed in plasma were the same as the mass spectra of reference standard.

Mass Spectra of M3. The deprotonated molecular ion of M3 was observed at m/z 563.3. Loss of glucuronic acid (–176 Da) from the m/z 563 gave the parent fragment ion at m/z 387. Cleavage at C-S bonds at various positions gave characteristic fragment ion at m/z 263 as discussed above for parent. The mass spectra and fragmentation ions of M3 observed in plasma were the same as the mass spectra of reference standard.

Mass Spectra of M4a and M4b. The protonated molecular ions of M4a and M4b were observed at m/z 377.1234 and 377.1226, respectively. These metabolites were proposed to be oxidative metabolites of M1 (+O). The fragment ions related to C-S cleavages at m/z 181, 91, and 237 indicated that the oxidation positions were on one of the benzyl moieties. The fragment ion at m/z 137 further indicated the oxidation was probably on the benzyl closer to the carboxylic acid.

Mass Spectra of M5a and M5b. The protonated molecular ions of M5a and M5b were observed at m/z 375.1079 and 375.1078, respectively. These metabolites were proposed to be oxidative metabolites (+O, –2H) of M1. The fragment ions related to C-S cleavages at m/z 181 and 213 indicated the oxidation position was on the aliphatic part of the molecule.

Mass Spectra of M6a and M6b. The protonated molecular ions of M6a and M6b were observed at m/z 393.1184 and 393.1186, respectively. These metabolites were proposed to be oxidative metabolites (+2O) of M1 based on the accurate mass. The fragment ions related to C-S cleavages at m/z 287, 253, and 161 indicated that one of the

oxidation positions was on the benzyl group and the other was on the aliphatic moieties. The oxidation position can be on either of the benzyl moieties.

Mass Spectra of M7. The deprotonated molecular ion of M7 was observed at m/z 535.4. This metabolite was proposed to be glucuronic acid conjugate of M1 based on the fragmentation pattern. Loss of glucuronic acid (–176 Da) from the m/z 535 gave the M1 fragment ion at m/z 359. Cleavage at C-S bonds at various positions gave characteristic fragment ions observed for M1.

Mass Spectra of M8. The deprotonated molecular ion of M8 was observed at m/z 551.4. The proposed fragmentation pathways of the mass spectra are shown in Table 3. This metabolite was proposed to be glucuronic acid conjugate of M4 based on the fragmentation pattern. Loss of glucuronic acid (–176 Da) from the m/z 551 gave the fragment ion at m/z 375 of M4.

Mass Spectra of M9. The deprotonated molecular ion of M9 was observed at m/z 416.4. This metabolite was proposed to be glycine conjugate of M1 based on the fragmentation pattern. Cleavage at C-S bonds gave fragment ions at m/z 292 and 156, suggesting the glycine conjugation of M1.

Mass Spectra of M10. The deprotonated molecular ion of M10 was observed at m/z 466.3. This metabolite was proposed to be taurine conjugate of M1 based on the fragmentation pattern. Cleavage of the amide bond gave fragment ion at m/z 342. Cleavage at C-S bonds gave fragment ions at m/z 284.

Mass Spectra of M11. The protonated molecular ion of M11 was observed at m/z 180.0657. Loss of H_2O from m/z 180 gave the fragment ion at m/z 162. The cleavage of the amide bond gave the fragment ion at m/z 105. The mass spectra and fragmentation ions of M11 observed in urine were the same as the mass spectra of reference standard hippuric acid.

Mass Spectra of M12. The protonated molecular ion of M12 was observed at m/z 409.1128. This metabolite was proposed to be an oxidative metabolite of M1 (+3O) based on the accurate mass. The fragment ion related to C-S cleavage at m/z 287 indicated that two of the oxidation positions were on the benzyl group and the other oxidation position was on the other side of the molecule. The oxidation could be on either of the benzyl groups.

Mass Spectra of M13. The protonated molecular ion of M13 was observed at m/z 425.1102. The accurate mass of M13 indicated an oxidative metabolite (+4O) of M1.

Mass Spectra of M14a and M14b. The protonated molecular ions of M14a and M14b were observed at m/z 391.1024 and 391.1022, respectively. Based on the fragmentation shown in Table 3, they were proposed to be oxidative metabolites of M1 (+2O, –2H).

Mass Spectra of M15. The protonated molecular ion of M15 was observed at m/z 301.0932. This metabolite was proposed to be an oxidative and methylated metabolite after S-dealkylation of M1. The fragment ions related to C-S cleavages at m/z 237 and 159 indicated the addition of CH_2O was on the aliphatic region of the molecule. The S-dealkylation could be on either sulfur atoms.

Metabolite Profile in Pooled Plasma, Urine, and Feces. The average recoveries of total radioactivity from pooled plasma, urine, and fecal sample extractions were about 95%. The average HPLC recovery for all matrices was about 98%, indicating that all injected radioactivity in samples were eluted by the HPLC method used in this study. Multiple peaks on HPLC with different retention times but with same molecular masses are numbered sequentially with alphabetical suffixes.

Representative radiochromatogram of pooled rat plasma samples (0–48 hours) is shown in Fig. 3. Unchanged parent compound accounted for about 18% of plasma radioactivity. Metabolites M1, M4a, and M5a derived from oxidative reactions were observed as major radioactive components and accounted for 9%, 18%, and 50% of

TABLE 3
Summary of key mass spectral data of CPI-613 and its metabolites in rat and human

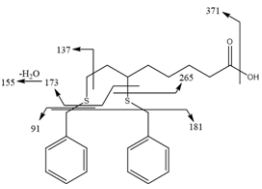
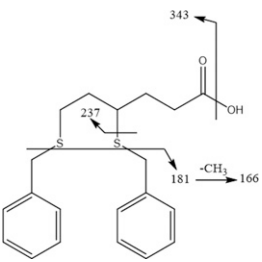
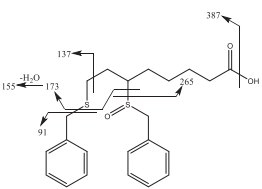
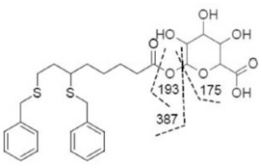
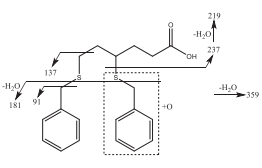
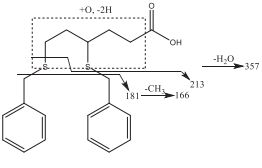
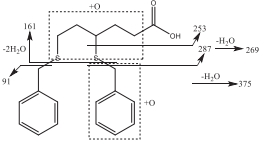
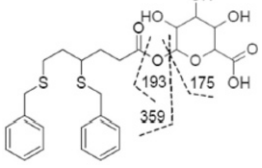
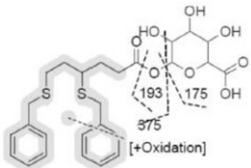
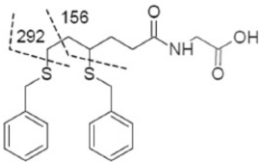
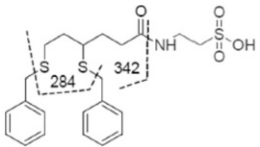
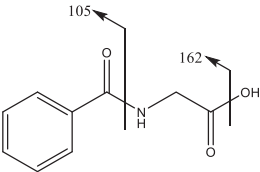
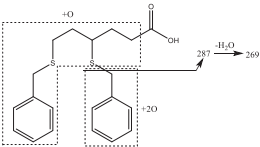
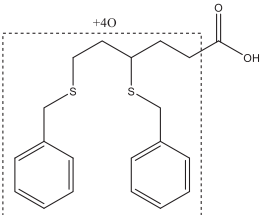
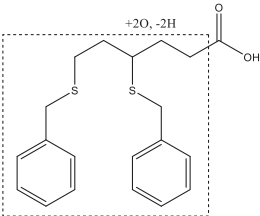
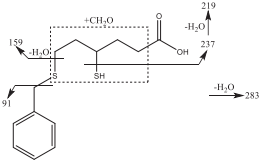
Parent or Metabolite	Structure and Proposed Fragmentation	[M + H] ⁺ or [M – H] [–]	Characteristic CID Fragmentation Ions
CPI-613		389.1603	371, 265, 181, 173, 91
M1		361.1285	343, 237, 181, 166
M2		405.1544	387, 265, 173, 155
M3		563.3	387, 263, 193, 175
M4a/b		377.1234, 377.1226	359, 237, 219, 181
M5a/b		375.1079, 375.1078	357, 213, 181, 166
M6a/b		393.1184	375, 287, 269, 253, 161
M7		535.4	359, 193, 175

TABLE 3 continued

Parent or Metabolite	Structure and Proposed Fragmentation	$[M + H]^+$ or $[M - H]^-$	Characteristic CID Fragmentation Ions
M8		551.4	460, 375, 193, 175
M9		416.4	292, 156
M10		466.3	342, 284
M11		180.0657	162, 105
M12		409.1128	287, 269
M13		425.1102	407, 349, 281, 237
M14a/b		391.1024, 391.1022	373, 355, 297, 285
M15		301.0932	283, 237, 219, 159

plasma total radioactivity, respectively. Oxidative metabolites M12 and M4b were detected as minor components, and each accounted for <2% of plasma radioactivity.

Representative radiochromatogram of pooled urine samples (90% pool) in rats is shown in Fig. 4. Unchanged parent compound was not observed in urine. The major metabolite found in urine was a polar

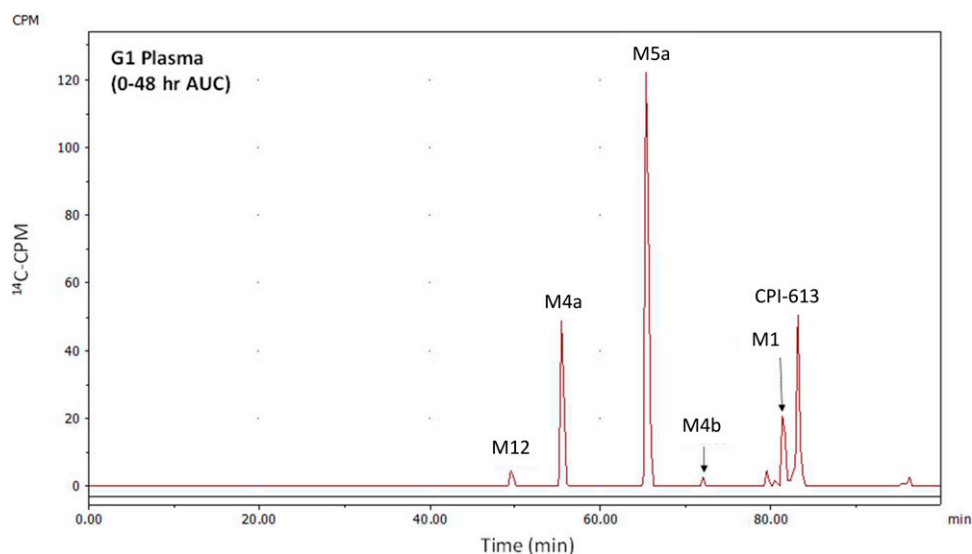


Fig. 3. HPLC radiochromatogram of rat plasma after a single i.v. infusion of 100 mg/kg (200 μ Ci/kg) [14 C] CPI-613 to SD rats. CPI-613 at 50 mg/ml in 1M TEA was diluted to 10 mg/ml (20 μ Ci/ml) with 5% dextrose in water (D5W) and infused at 5 ml/h per kg for 2 hours. Plasma pooled (0–48 hours) from four rats was extracted with acetonitrile followed by LC-MS analysis with radiometric detection.

metabolite M11 (~58% of urine radioactivity and ~11% of the dose) with retention time at ~9.9 minutes. M11 was identified as hippuric acid, which could be derived from oxidation at the benzylic carbon, hydrolysis, followed by glycine conjugation. In addition, oxidative metabolites M6a, M6b, and M12, derived from M1, were observed in relatively small amounts (<3% of the dose).

Representative radiochromatogram of pooled fecal samples (90% pool) in rats is shown in Fig. 5. Unchanged parent compound was observed and accounted for ~6% of fecal radioactivity or ~3% of the dose. M1 was found as the major radioactive peak in fecal extract and accounted for ~24% of fecal radioactivity and ~13% of the dose.

Additional metabolites detected in the feces (M4a, M4b, M5a, M5b, M13, and M14) were formed after further oxidation of M1.

CPI-613 Metabolites in Human Plasma. Fig. 6 shows the extracted ion chromatogram of metabolites identified in pooled human plasma. Unchanged parent compound accounted for about 3.7% of the AUC. The β -oxidation product M1 constituted the major metabolite circulating at 38%. Other major metabolites identified were those derived from M1, including M4a (+O, 20%), M4b (+O, 7.4%), M5a (+O-2H, 23%), and M7 (glucuronic acid conjugate of M1, 7%). Minor metabolites (<0.5% of the AUC) included M8 (glucuronic acid conjugate of M1 + O), M9 (glycine conjugate of M1), M10 (taurine conjugate of

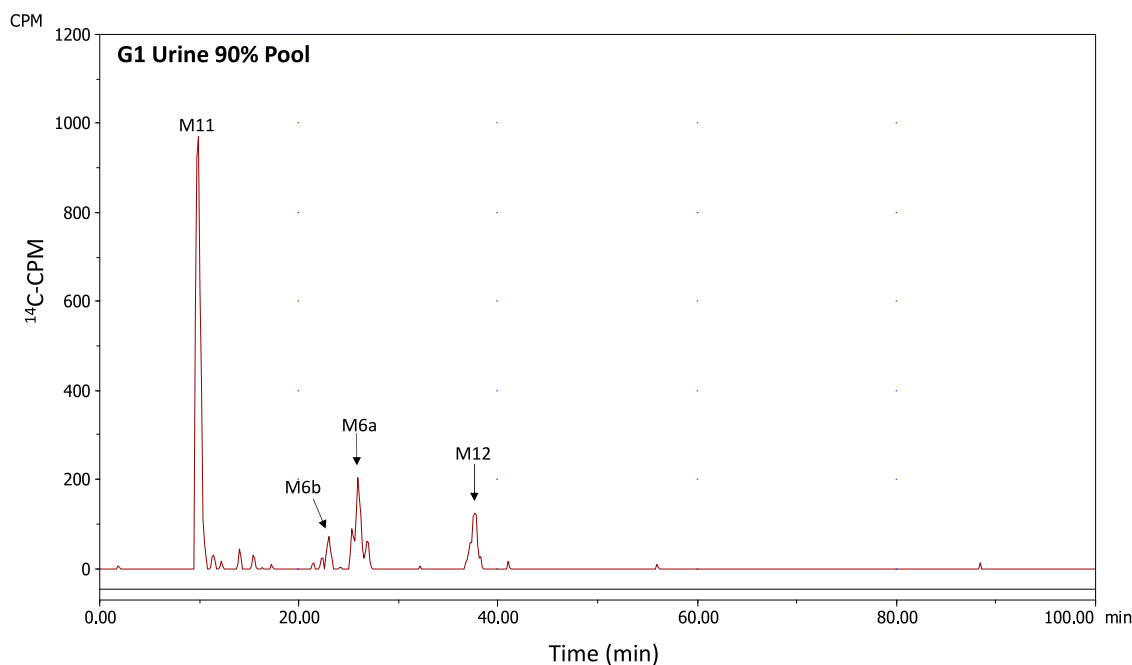


Fig. 4. HPLC radiochromatogram of rat urine after a single i.v. infusion of 100 mg/kg (200 μ Ci/kg) [14 C] CPI-613 to SD rats. CPI-613 at 50 mg/ml in 1M TEA was diluted to 10 mg/ml (20 μ Ci/ml) with D5W and infused at 5 ml/h per kg for 2 hours. Urine pooled (90% pool) from four rats was mixed with acetonitrile and centrifuged, and the supernatant was analyzed by LC-MS with radiometric detection.

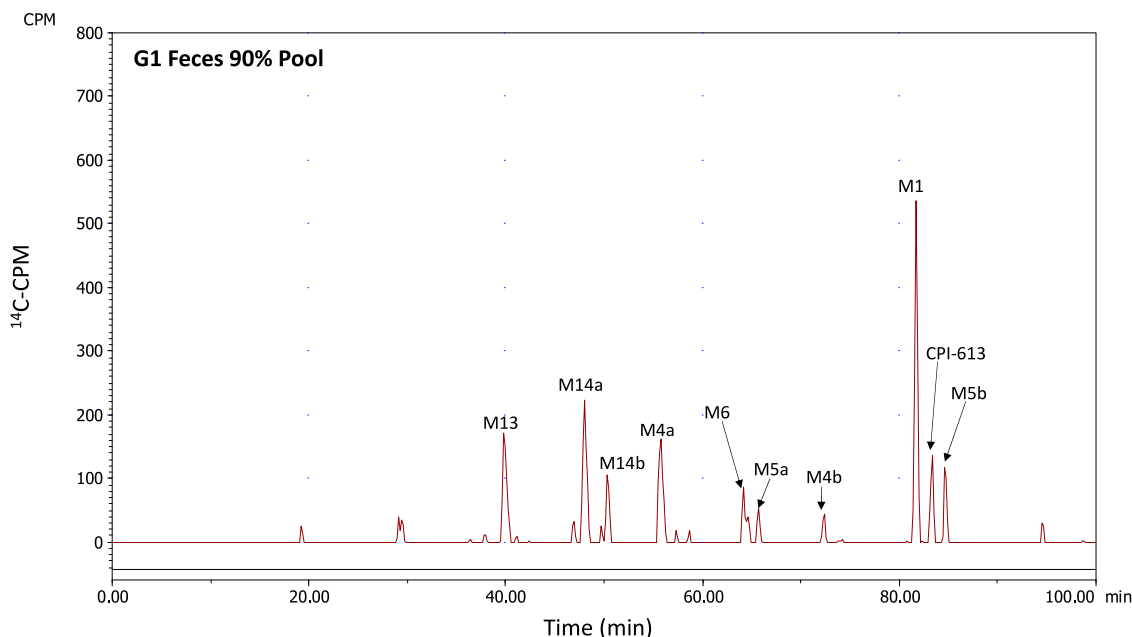


Fig. 5. HPLC radiochromatogram of rat feces after a single i.v. infusion of 100 mg/kg (200 μ Ci/kg) [14 C] CPI-613 to SD rats. CPI-613 at 50 mg/ml in 1M TEA was diluted to 10 mg/ml (20 μ Ci/ml) with D5W and infused at 5 ml/h per kg for 2 hours. Fecal samples pooled (90% pool) from four rats were extracted with acetonitrile followed by LC-MS analysis with radiometric detection. Multiple metabolites with the same mass are given the same M number with alphabetical suffix.

M1), M2 (parent sulfoxide), and M3 (parent glucuronic acid conjugate). Minor metabolites are not shown in the figure for clarity.

Kinetics of CPI-613 Metabolism in Human Hepatocytes and Fraction Metabolized. The objective of this study was to determine the Michaelis-Menten kinetics (V_{\max} and K_m) of the metabolism of CPI-613 to M1 (β -oxidation), M2 (sulfoxidation), and M3 (glucuronidation) in cryopreserved human hepatocytes. Preliminary experiments showed that these three were the major metabolites formed in human hepatocytes (data not shown). The overall goal was to obtain information about the fraction of CPI-613 metabolized (f_m) by each pathway/enzyme by comparing the intrinsic clearance (CL_{int}) values obtained in the study.

For evaluation of the formation kinetics of M1, M2, and M3, optimum conditions with respect to incubation time and hepatocytes

concentration were first established (data not shown). After this, the kinetic studies were performed using human hepatocytes at a density of 0.4 million cells/ml and incubation time of 135 minutes, under which the formation of M1, M2, and M3 was linear as well as high enough for kinetic evaluation. Concentrations of M1, M2, and M3 in extracts of human hepatocytes incubations were determined using a qualified LC-MS/MS method.

The formation of M1 showed saturable kinetics, which was amenable to facile determination of V_{\max} and K_m by plotting velocity of M1 formation against CPI-613 concentrations (Fig. 7). The formation of M2 and M3 also showed saturable kinetics, although inclusion of higher substrate concentrations would have resulted in better saturation curves (Fig. 7). However, this could not be done due to what appears to be the cytotoxic effect of CPI-613 at the 500 and 1000 μ M concentrations.

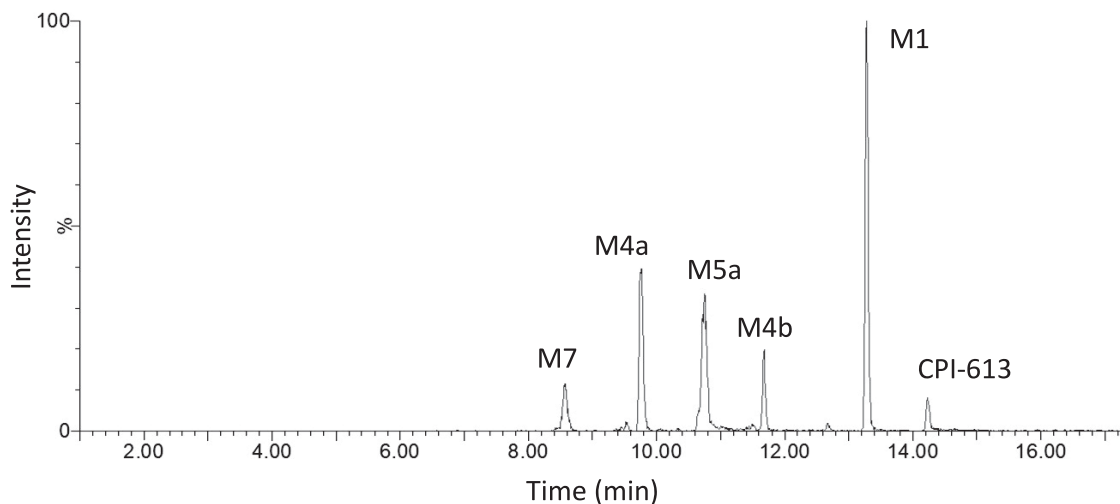


Fig. 6. Representative extracted ion chromatogram of pooled human plasma samples after a single i.v. infusion of 2940 mg/kg CPI-613 ($n = 1$). CPI-613 dosing solution was prepared from 50 mg/ml in 1M TEA diluted with D5W and infused i.v. at 2.3 ml/min for 2 hours. Equal volumes of plasma extracts with ACN at 0.5, 6, and 24 hours (postinfusion) were pooled and analyzed by LC-MS.

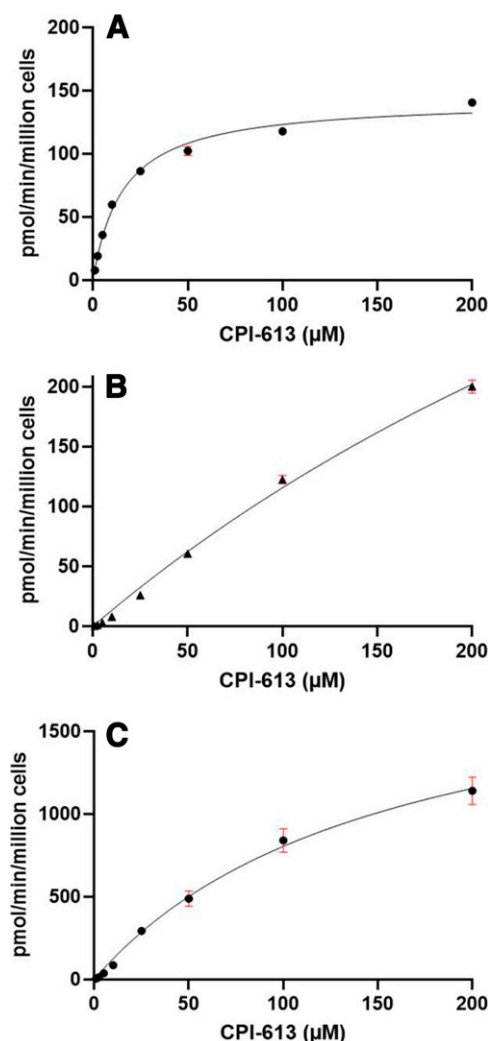


Fig. 7. Michaelis-Menten plots (V vs. $[S]$) of β -oxidation product M1 (A), sulfoxide M2 (B), and glucuronide M3 (C) formed from CPI-613 in human hepatocytes. Incubation mixtures of hepatocytes with CPI-613 were extracted with ACN and centrifuged, and the metabolites in the supernatants were quantitated by LC-MS.

The ratio of V_{\max} to K_m (CL_{int}) was 8.92, 1.35, and 13.32 $\mu\text{L}/\text{min}$ per million cells for the formation of M1, M2, and M3 in human hepatocytes, respectively. Thus, the fraction metabolized (f_m) via the metabolic route leading to M1, M2, and M3 was estimated to be 38%, 6%, and 56%, respectively. The kinetic parameters obtained are shown in Table 4.

CPI-613 Metabolites in Human Liver Microsomes. The objective of this study was to determine the extent of metabolism of CPI-613 in vitro using liver microsomes and NADPH and to estimate the amount of M1 and M2 formed. CPI-613 was metabolized quickly and extensively in both species with a half-life of 25–38 minutes in rat and 10–21 minutes in human. With incubation of 1 and 10 μM CPI-613, the highest mean concentration of M2 was 0.3 and 4 μM in both species, respectively. M1 was also monitored but was not detected in liver microsomes from both species.

CPI-613 Metabolites in Human Liver Mitochondria. The objective of this study was to determine the metabolite profile of CPI-613 in human liver mitochondria, particularly whether M1 was formed after the presumed β -oxidation. Figure 8 shows the representative LC-MS profile of extracts of CPI-613 (100 μM) incubations with human liver mitochondria and cofactors required for β -oxidation. Data showed that CPI-613 was metabolized to M1. In addition, an oxidized derivative of M1 (M4a/

TABLE 4

Michaelis-Menten kinetic parameters of metabolites M1, M2, and M3 formation after incubation of CPI-613 with human hepatocytes

Metabolite	V_{\max} (pmol/min per million cells)	K_m (μM)	CL_{int} ($\mu\text{L}/\text{min}$ per million cells)	f_m (%)
M1	142.9 ± 1.03	16.02 ± 0.60	8.92 ± 0.272	38
M2	816.5 ± 149.8	607.4 ± 130.7	1.35 ± 0.059	6
M3	2117 ± 399.3	164.4 ± 54	13.32 ± 2.082	56

b, 376 Da) was also detected in small amounts. M1 and M4a/b were formed in a cofactor-dependent manner. Thus, it was concluded that M1 and M4a/b are liver mitochondrial β -oxidation metabolites of CPI-613.

Discussion

The objective of the present study was to evaluate the disposition of CPI-613 in rats as well as to identify the metabolic pathways in human and determine whether the metabolites are adequately tested for safety in preclinical species. Thus, rats were infused intravenously (intended clinical route of administration) with CPI-613 at the maximum tolerated dose of 100 mg/kg. After intravenous infusion for 2 hours, radioactivity was excreted slowly and only about 81% of the administered radioactivity was recovered by 168 hours. Radioactivity in the carcasses accounted for an additional 5.5%. Therefore, to recover the remaining radioactivity, a separate study was conducted to investigate the radioactivity in the expired air. Since hippuric acid was identified as a metabolite in the urine (see discussion below), the likely benzoic acid intermediate may undergo oxidation to release CO_2 . Oxidative decarboxylation of benzoic acid to CO_2 by rat liver microsomes has been reported (Winston and Cederbaum, 1982). In the present study, data showed that radioactivity excreted in the expired air was a small amount (2.3%), bringing the total recovery of radioactivity to 88.3%. Based on the observation that the radioactivity was excreted slowly and that the amount of radioactivity excreted on day 7 alone was still significant at $\sim 3\%$, it is reasonable to conclude that the CPI-613-derived radioactivity would be completely excreted eventually, as was later confirmed by quantitative whole-body autoradiography study. By 504 hours, radioactivity was not detectable in any tissue, bile, blood, urine, or alimentary canal contents (data not shown).

The major circulating components in rat plasma were the parent, M1, M4a, M4b, and M5a. M1 was formed via β -oxidation of CPI-613, and M4a, M4b, and M5a are the further oxidized metabolites of M1. A qualitatively similar metabolite profile was observed in human plasma. However, although M1 was the predominant component in human plasma, it was rapidly further metabolized to M5a in rats (see discussion below). The major metabolites circulating in human plasma were also detected in rat plasma.

[^{14}C]-CPI-613 was primarily eliminated via oxidative metabolism in rats followed by excretion of metabolites in feces (59%) and urine (22%). Major metabolite in rat feces was the β -oxidation product M1. Urine had a distinct metabolism profile, hippuric acid (M11) being the major metabolite. M11 was likely formed after the oxidation at the benzylic carbon (the carbon atom between sulfur and phenyl ring), which upon hydrolysis may form benzoic acid and subsequently undergo conjugation with glycine. Other smaller peaks in the feces and urine constituted multiple minor oxidative metabolites derived from the β -oxidation product M1. These data suggest that CPI-613 is cleared primarily via β -oxidation in rats, whereas other routes of clearance (i.e., sulfur oxidation and benzylic oxidation) were minor pathways.

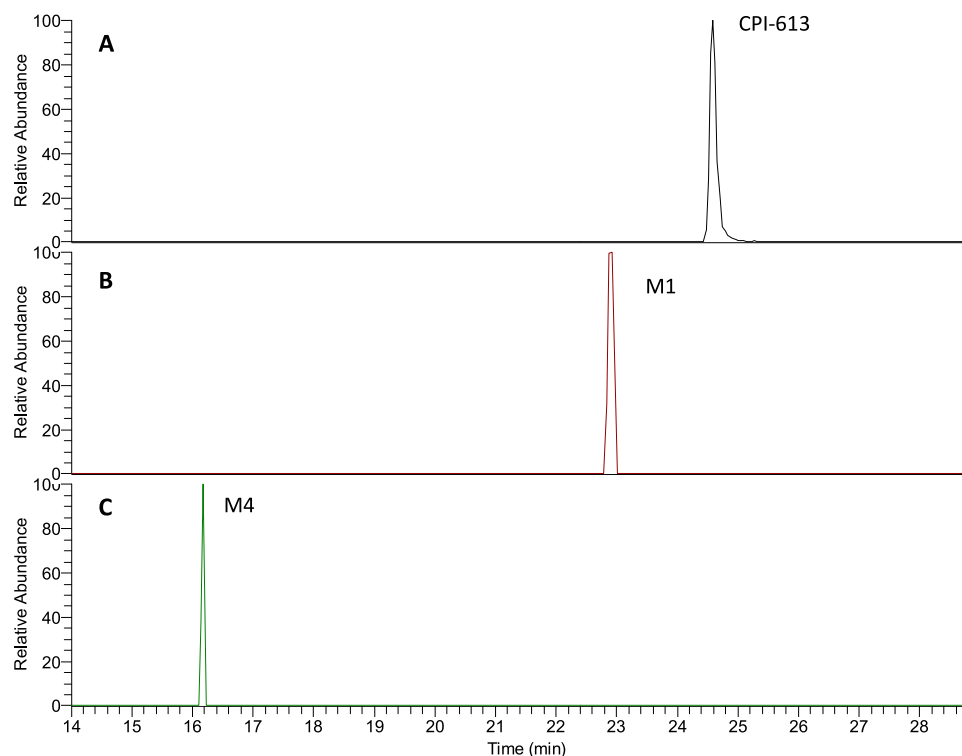


Fig. 8. Extracted ion chromatograms after incubation of CPI-613 with human liver mitochondria: (A) CPI-613 remaining; (B) M1 formed after β oxidation; and (C) M4a/b, an oxidative (+O) product of M1. The reaction mixture contained CPI-613 (100 μ M) pooled human liver mitochondria (5 mg/ml), phosphate buffer (0.1 M, pH 7.4), ATP (5 mM), CoASH (0.1 mM), L-carnitine (2 mM), and MgCl₂ (3 mM). After 2 hours incubation, the mixtures were extracted with ACN and centrifuged, and the metabolites in the supernatants were quantitated by LC-MS.

The metabolism and excretion routes of CPI-613 make an interesting comparison with those of its endogenous counterpart lipoic acid. Lipoic acid is reported to be extensively metabolized via β -oxidation pathway (Schupke et al., 2001; Teichert et al., 2003; 2005). Since CPI-613 is an analog of lipoic acid, it was not surprising that CPI-613 was also cleared primarily via β -oxidation pathway (Fig. 9). CPI-613, similar to that reported for lipoic acid, underwent rapid β -oxidation and the metabolites appeared in the plasma within a few minutes after drug administration. The rapid appearance of these metabolites in plasma highlights the fact that the β -oxidation of these compounds proceeds very effectively, especially in the liver mitochondria (Adeva-Andany et al., 2019). It appears that CPI-613 β -oxidation capability is relatively more pronounced in rats compared with that in humans as M1 was the major circulating component in human plasma, whereas in rats M1 was further oxidized to M5a and M5b. M5a/b is likely the β -keto metabolite formed during the course of β -oxidation of M1. The β -oxidation capability of lipoic acid is variable across species. Lipoic acid, with or without the reduction of the disulfide bond, underwent two cycles of β -oxidation steps in dogs and humans (Schupke et al., 2001; Teichert et al., 2003, 2005). As soon as 10 minutes after the intravenous dosing of lipoic acid, tetranorlipoic acid, the final product of β -oxidation, was the major component of the radioactivity in dog and human plasma. Conversely, in rat plasma, products of lipoic acid after the first cycle of β -oxidation and intermediates that form during the second cycle of β -oxidation were observed, similar to the products of CPI-613 observed in the current study (Fig. 9). Regarding excretion, lipoic acid metabolites were excreted mainly in the urine in all species (Schupke et al., 2001). In contrast, in the present study in rats, the majority of CPI-613-related radioactivity was excreted in the feces.

In incubations with human liver S9, CPI-613 was mainly metabolized to sulfoxide (M2) and glucuronide (M3). Several cytochrome P450

(P450) isoenzymes were capable of sulfur oxidation in CPI-613 (Lee et al., 2011). As expected, M1 was not observed in liver S9 incubations since β -oxidation of fatty acids is a mitochondrial reaction (Adeva-Andany et al., 2019). In the present study, human liver mitochondria were used to explore the in vitro β -oxidation of CPI-613. Data showed that CPI-613 was converted to M1 after the first cycle of β -oxidation. In addition, M4a/b was also identified in small amounts. However, unlike lipoic acid metabolism in dogs, the reaction did not progress to the second cycle of β -oxidation. It is possible that the benzyl groups on sulfur atoms provide steric hindrance, preventing completion of the final cycle of CPI-613 β -oxidation. This in vitro reaction observation agrees with the metabolite profile observed in rat excreta. Although CPI-613 was rapidly metabolized to M1, further metabolism of M1 was slow and it was mainly eliminated as oxygenated metabolites that are not related to β -oxidation in rats.

We investigated the clearance routes of CPI-613 in humans using hepatocytes. The purpose of this study was also to estimate the extent of P450-mediated metabolism and inform on the implications for drug interactions when coadministered drugs are P450 inhibitors. Preliminary studies in hepatocyte incubations with CPI-613 identified M1, sulfoxide (M2), and glucuronic acid conjugate (M3), as major metabolites. Following this information, Michaelis-Menten kinetics (V_{\max}/K_m) of the metabolism of CPI-613 to these three metabolites was conducted. Data showed that glucuronidation was the major route of clearance for CPI-613 in human hepatocytes. The fraction metabolized (f_m) via the metabolic route leading to parent glucuronide was estimated to be 56%, followed by β -oxidation at 38% and sulfur oxidation at 6%. In a preliminary pharmacokinetic study of CPI-613 in humans where plasma samples were collected up to 72 hours, PK profiles showed prominent secondary peaks, suggesting enterohepatic recirculation likely due to the metabolite M3, the glucuronic acid conjugate of CPI-613 (Pardee et al.,

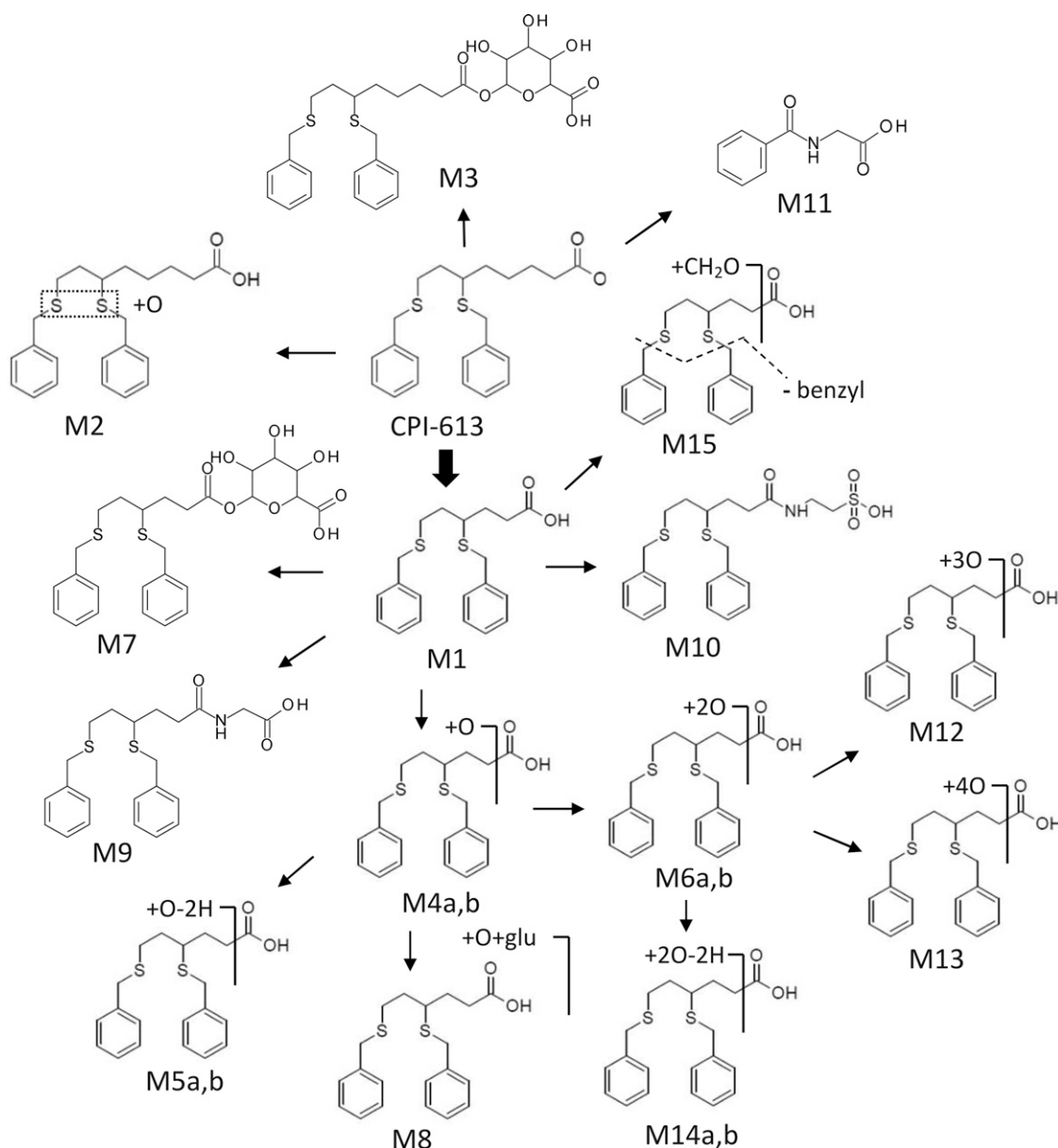


Fig. 9. Proposed metabolic pathways of CPI-613 in rats and humans.

2014). However, M3 was detected circulating in human plasma only in trace amounts. For comparison, in a rat PK study, there was a slight indication of enterohepatic circulation, particularly at doses >100 mg/kg (data not shown), but M3 was not detected in plasma or feces. It is possible that the parent detected in rat feces was a result of hydrolysis of M3 back to the parent. Finally, intrinsic clearance analysis in human hepatocytes suggests that, since contribution of P450-mediated metabolism toward total clearance is small, CPI-613 is unlikely to be a victim of drug-drug interactions as a result of P450 inhibition by coadministered drugs. Valproic acid, a widely used drug for the treatment of epilepsy, is also reported to be cleared via glucuronidation, β -oxidation, and P450-mediated oxidation similar to CPI-613 (Silva et al., 2008). However, unlike valproic acid, there is no indication of interference of CPI-613 with endogenous mitochondrial β -oxidation leading to toxicities in human, which is a subject matter of another manuscript in preparation.

In conclusion, CPI-613 metabolite profiles in rat and human plasma were qualitatively similar. The majority of the [^{14}C]-CPI-613-related

radioactivity was excreted within a week in feces (59%) and urine (22%) in rats. The metabolites were mainly formed after β -oxidation. The β -oxidation reaction occurred in mitochondria, and the resulting metabolite M1 rapidly appeared in rat and human plasma. Studies conducted in hepatocytes suggested glucuronidation and β -oxidation as the major clearance mechanisms in humans. In both rats and humans, CPI-613 rapidly undergoes the first cycle of β -oxidation; however, unlike endogenous lipoic acid, it does not proceed to completion of the final β -oxidation step, likely due to steric hindrance from bulky benzyl groups on sulfur atoms.

Authorship Contributions

Participated in research design: V.B. Reddy, Shen, Kassahun, Hu.
Conducted experiments: A. Boteju, Shen, Kassahun, N. Reddy.
Contributed new reagents or analytical tools: L. Boteju.
Performed data analysis: V.B. Reddy, A. Boteju, Shen, Kassahun, N. Reddy, Sheldon.
Wrote or contributed to the writing of the manuscript: V.B. Reddy, Luther, Hu.

References

- Adeva-Andany MM, Carneiro-Freire N, Seco-Filgueira M, Fernández-Fernández C, and Mourinho-Bayolo D (2019) Mitochondrial β -oxidation of saturated fatty acids in humans. *Mitochondrion* **46**:73–90.
- Alistar A, Morris BB, Desnoyer R, Klepin HD, Hosseinzadeh K, Clark C, Cameron A, Leyendecker J, D'Agostino Jr R, Topaloglu U, et al. (2017) Safety and tolerability of the first-in-class agent CPI-613 in combination with modified FOLFIRINOX in patients with metastatic pancreatic cancer: a single-centre, open-label, dose-escalation, phase 1 trial. *Lancet Oncol* **18**:770–778.
- Bingham PM, Stuart SD, and Zachar Z (2014) Lipoic acid and lipoic acid analogs in cancer metabolism and chemotherapy. *Expert Rev Clin Pharmacol* **7**:837–846.
- DeBerardinis RJ and Chandel NS (2016) Fundamentals of cancer metabolism. *Sci Adv* **2**:e1600200.
- Hammoudi N, Ahmed KB, Garcia-Prieto C, and Huang P (2011) Metabolic alterations in cancer cells and therapeutic implications. *Chin J Cancer* **30**:508–525.
- Kassahun K, Hu P, Grillo MP, Davis MR, Jin L, and Baillie TA (1994) Metabolic activation of unsaturated derivatives of valproic acid. Identification of novel glutathione adducts formed through coenzyme A-dependent and -independent processes. *Chem Biol Interact* **90**:253–275.
- Lee KC, Shorr R, Rodríguez R, Maturo C, Boteju LW, and Sheldon A (2011) Formation and anti-tumor activity of uncommon in vitro and in vivo metabolites of CPI-613, a novel anti-tumor compound that selectively alters tumor energy metabolism. *Drug Metab Lett* **5**:163–182.
- Missirolis S, Perrone M, Genovese I, Pinton P, and Giorgi C (2020) Cancer metabolism and mitochondria: finding novel mechanisms to fight tumours. *EbioMedicine* **59**:102943.
- Pardee TS, Anderson R, Miller LD, Pladna KM, Isom S, Ellis LR, Berenzon D, Howard DS, Hurd DD, Manuel M, et al. (2016) TCA cycle inhibition by CPI-613 increases sensitivity to chemotherapy in older and poor risk acute myeloid leukemia, in Proceedings of the American Society of Hematology Annual Meeting; 2016 December 3–6; San Diego, CA. American Society of Hematology, Washington, DC.
- Pardee TS, Lee K, Luddy J, Maturo C, Rodriguez R, Isom S, Miller LD, Stadelman KM, Levitan D, Hurd D, et al. (2014) A phase I study of the first-in-class antimetabolic agent, CPI-613, in patients with advanced hematologic malignancies. *Clin Cancer Res* **20**:5255–5264.
- Pardee TS, Luther S, Buyse M, Powell BL, and Cortes J (2019) Devimistat in combination with high dose cytarabine and mitoxantrone compared with high dose cytarabine and mitoxantrone in older patients with relapsed/refractory acute myeloid leukemia: ARMADA 2000 phase III study. *Future Oncol* **15**:3197–3208.
- Philip PA, Buyse ME, Alistar AT, Rocha Lima CM, Luther S, Pardee TS, and Van Cutsem E (2019) A phase III open-label trial to evaluate efficacy and safety of CPI-613 plus modified FOLFIRINOX (mFFX) versus FOLFIRINOX (FFX) in patients with metastatic adenocarcinoma of the pancreas. *Future Oncol* **15**:3189–3196.
- Potchoiba MJ, Tensfeldt TG, Nocerini MR, and Silber BM (1995) A novel quantitative method for determining the biodistribution of radiolabeled xenobiotics using whole-body cryosectioning and autoradioluminography. *J Pharmacol Exp Ther* **272**:953–962.
- Schupke H, Hempel R, Peter G, Hermann R, Wessel K, Engel J, and Kronbach T (2001) New metabolic pathways of α -lipoic acid. *Drug Metab Dispos* **29**:855–862.
- Silva MFB, Aires CCP, Luis PBM, Ruiter JPN, Ijst L, Duran M, Wanders RJA, and Tavares de Almeida I (2008) Valproic acid metabolism and its effects on mitochondrial fatty acid oxidation: a review. *J Inher Metab Dis* **31**:205–216.
- Stuart SD, Schauble A, Gupta S, Kennedy AD, Keppler BR, Bingham PM, and Zachar Z (2014) A strategically designed small molecule attacks α -ketoglutarate dehydrogenase in tumor cells through a redox process. *Cancer Metab* **2**:4.
- Teichert J, Hermann R, Ruus P, and Preiss R (2003) Plasma kinetics, metabolism, and urinary excretion of α -lipoic acid following oral administration in healthy volunteers. *J Clin Pharmacol* **43**:1257–1267.
- Teichert J, Tuemmers T, Achenbach H, Preiss C, Hermann R, Ruus P, and Preiss R (2005) Pharmacokinetics of α -lipoic acid in subjects with severe kidney damage and end-stage renal disease. *J Clin Pharmacol* **45**:313–328.
- Vander Heiden MG (2011) Targeting cancer metabolism: a therapeutic window opens. *Nat Rev Drug Discov* **10**:671–684.
- Winston GW and Cederbaum AI (1982) Oxidative decarboxylation of benzoate to carbon dioxide by rat liver microsomes: a probe for oxygen radical production during microsomal electron transfer. *Biochemistry* **21**:4265–4270.
- Zachar Z, Marecek J, Maturo C, Gupta S, Stuart SD, Howell K, Schauble A, Lem J, Piramzadian A, Kamik S, et al. (2011) Non-redox-active lipoate derivatives disrupt cancer cell mitochondrial metabolism and are potent anticancer agents in vivo. *J Mol Med (Berl)* **89**:1137–1148.

Address correspondence to: Vijay Bhasker Reddy, Rafael Pharmaceuticals, 1 Duncan Drive, Cranbury, NJ 08512-3643. E-mail: vijay.reddy@rafaelpharma.com